ISSN 2079-0864, Biology Bulletin Reviews, 2018, Vol. 8, No. 5, pp. 406–420. © Pleiades Publishing, Ltd., 2018.
Published in Russian in Zhurnal Obshchei Biologii, 2017, Vol. 78, No. 5, pp. 63–80.

How Long Does a Short-Lived Perennial Live? A Modeling Approach[1]

D. O. Logofet[a], *, E. S. Kazantseva[b], **, I. N. Belova[a], and V. G. Onipchenko[b], ***

[a]Laboratory of Mathematical Ecology, Institute of Atmospheric Physics, Russian Academy of Sciences,
Moscow, 119017 Russia
[b]Biological Department, Moscow State University, Moscow, 119234 Russia
**e-mail: danilal@postman.ru*
***e-mail: biolenok@mail.ru*
****e-mail: vonipchenko@mail.ru*

Received April 5, 2017

Abstract—We have composed a "scale of ontogenesis," i.e., the sequence of ontogenetic stages, and the life cycle graph (LCG) for *Androsace albana,* a monocarpic plant species that is considered a short-lived perennial, according to annual observations on permanent sample plots in an alpine lichen heath during the 2009–2016 period. There is only one reproduction event in the LCG, which eliminates any reproductive uncertainty from the data of "identified individuals" type so typical for the former projects with polycarpic species, while the monocarpic cycle excludes any returns from the generative stage to a non-flowering status. The LCG describes the ontogeny through five successive stages: seedlings, juvenile, immature, adult virginal, and generative plants, the generative plants perishing after they have flowered and produced seeds. We have constructed a matrix model of the stage-structured population that corresponds to the LCG; its calibration has reduced to calculating the vital rates directly from the data of one time step, i.e., from the censuses at two successive years of observation. Therefore, the nonautonomous model represents a set of 7 annual matrices, each giving a quantitative measure of how the local population is adapted to its environment as the dominant eigenvalue of the model matrix. Its variations have turned out quite significant from year to year, signifying either a growth or decline of the local population and, in general, its vulnerability to stress factors of the environment. Averaging the annual matrices geometrically over the whole observation period has revealed the tendency to decline and enabled us to extract certain age-specific traits (in years) from the stage-structured model using the technique of virtual absorbing Markov chains and their fundamental matrices. The mean life expectancy at various stages of the *A. albana* ontogeny has turned out maximal in the adult virginal plants, while the mean age at flowering equal to 13 years has exceeded the horizon of the observation time series, thus proving the technique to be efficient. The model indicates that *A. albana* plants spend most of their life spans as virginal adults, which characterizes the *space holder* strategy by Körner (2003), or the *delayed-development* strategy by Zhukova (1995). The model outcome gives another evidence that the *A. albana* population is endangered.

DOI: 10.1134/S2079086418050043

INTRODUCTION

The issue of biodiversity studies and conservation is among the urgent ones (*Sovremennye podkhody*..., 2008). Applied to plant communities, the methods of population analysis provide for reliable ways to the monitoring, diagnosing, and examining efficiently the local population status of economically valuable, fodder, melliferous, and medicinal plant species (including rare ones) in natural and artificial communities (*Dinamika tsenopopulyatsii*..., 1985; Zhukova, 1995; Mirkin and Naumova, 1998; *Populyatsionnaya ekologiya*..., 2003). To solve a number of theoretical and practical issues we need at least an approximate knowledge of how long the plants can live in the local communities, as well as how long certain periods of their life spans can last (Molisch, 1938; Rabotnov, 1946; Witte and Stöcklin, 2010). The long-lasting monitoring of marked plants enables the most accurate estimation of plant age (Rabotnov, 1946; *Polevaya geobotanika*, 1960; *Polivariantnost' razvitiya*..., 2006). However, given that the life span of plants can be extremely long, researchers often resort to mathematical modeling, which makes it possible to calculate the life span duration from the data on short-term observations of the age and mortality in a large number of individual plants (Onipchenko, 2013). *Matrix models* of single-species, age-structured population dynamics were first introduced by Bernardelli (1941), Lewis

---

[1] The article was translated by the authors.

(1942), and Leslie (1945); in the current studies, their stage-structured generalizations are used everywhere (Salguero-Gomez et al., 2015), and to this day, they are a source of new mathematical problems and motivate developing new analytical methods (Crone et al., 2011, 2013; Logofet, 2013c; Logofet et al., 2017a, 2017b).

Following Zhmylev et al. (2005), the "short-lived plants," or "short-lived perennials" are mono- or polycarpic plants whose life spans range from 1 to 15 years. As noted by Zhukova (1995), the short-lived perennials may serve as convenient model objects since they feature the short complete ontogeny.

Androsace albana Stev. is presumably a short-lived perennial typical of the Alpine plant communities in the Caucasus. This species was studied by the generally accepted method of studying local populations in a natural habitat on permanent plots (Rabotnov, 1950a, 1950b).

In the world and national literature, so-called *matrix models* have long and fruitfully been used to describe the dynamics of single-species, discrete-structured populations, see the reviews in Caswell (2001), Logofet and Belova (2008), and Logofet et al. (2016). The dominant eigenvalue, $\lambda_1(\boldsymbol{L})$, of the model matrix $\boldsymbol{L}$ serves as the *adaptation measure* of the local population where and when the data have been mined to *calibrate* (i.e., to estimate quantitatively the elements of) matrix $\boldsymbol{L}$ (Logofet et al., 2014). Thus, the model is an effective tool for comparative plant demography (Logofet et al., 2014).

Normally, the data taken at two consecutive censuses are sufficient to calibrate matrix $\boldsymbol{L}$ (Caswell, 2001; Logofet, 2008, 2010), but we also have a longer series of observations in this project. Accordingly, we get several matrices, each depending on the time moment observation (a *nonautonomous* model). In the nonautonomous case, the range of tasks expands as compared to those solved traditionally for the autonomous model. In particular (after solving the calibration problem), the problem arises to estimate the measure of adaptation over the whole period of observations, and this problem is solved by averaging the annual matrices in a special way.

In this study, which continues a series of articles on the modeling of local single-species populations with a stage structure (Logofet et al., 2017a, 2017b, 2017c), we also consider the task to extract certain "age-specific traits [*in years*] from state-specific models" (Caswell, 2001, p. 116), in particular, we estimate the *life expectancy* for individuals in the local population and *the age at first flowering*, after averaging the model over the entire observation period. Thus, the characterization of the species in terms of short- vs. long-lived perennial becomes quantitatively certain.

MATERIALS AND METHODS

Object

Androsace albana Stev. is a herbaceous biennial tap-root monocarpic species (Shishkin and Bobrov, 1952; Shkhagapsoev, 1999). According to our data, *A. albana* manifests itself in the alpine lichen heaths as a herbaceous chamaephyte, summer-green, tap-root, monocarpic perennial. The species is included into *The Red Data Book of the Krasnodar Krai* (*Krasnaya kniga Krasnodarskogo*..., 2007) and *The Red Data Book of the Adygea Republic* (*Krasnaya kniga Respubliki Adygeya*..., 2012). This heliophilous species grows in alpine meadows, screes and stony places, cracks in limestone rocks and boulders in the subalpine, alpine, and subnival belts at the altitudes of 1800–3600 m (Shishkin and Bobrov, 1952; Grossheim, 1967; Shetekauri, 1998; Zernov, 2006, 2015).

In Teberda State Biosphere Reserve, *A. albana* is occasionally found on stony places and screes in the Alpine belt at the altitude of 2400–3040 m (Onipchenko et al., 2011); it has a narrow ecological amplitude in the altitude niche (with a range less than 400 meters, 2501–2900 m asl), tends to open communities with poor plant cover (the cover of the field layer is 31–50%), with the lichen cover more than 30%; the species was not recorded in communities with lichen covers more than 70% and less than 10%. It prefers well-illuminated habitats, slopes of the southern exposition less than 15° steep (Egorov et al., 2012; Egorov, 2015). Anthecology parameters of the species under the conditions of studied alpine community: actinomorphic flowers with wheel-shaped red corolla directed upward; located at the height of 100 ± 24 mm (mean ± standard deviation); the flowering duration per flower is 5.3 ± 1.7 (mean ± S.D.) days, per generative shoot 14 ± 3.4 days, per plant 15.2 ± 2.6 days. The species is part of the communities in alpine lichen heaths, Festuca varia grasslands of the alpine and subalpine belts, dwarf shrub heaths (Onipchenko, 2002).

Ontogeny of Androsace albana Stev. (Kazantseva, 2016)

Seeds are trihedral, irregular in shape, 2–3 mm long, 1 mm wide. Seed coat is papillose; color varies from red to fulvous-brown. After 5–6-month stratification, seeds sprout on the 12–22nd day after the germination has started.

Plantules. Germination is epigeal. The plantule is of rosette type with two cotyledons and two leaves. Cotyledons are green, oblong-ovate, drawn at the base, with a rounded apex, 7 mm long and 2 mm wide. The leaves are pointedly elliptical, 3 mm long and 2 mm wide, the leaf margin is ciliate. The hypocotyl is red or reddish-brown in color, 7 mm long. The main root is about 1.5 cm long (Fig. 1).

Juvenile plants. The cotyledons die off after 1–1.5 month after germination. The plant is a rosette

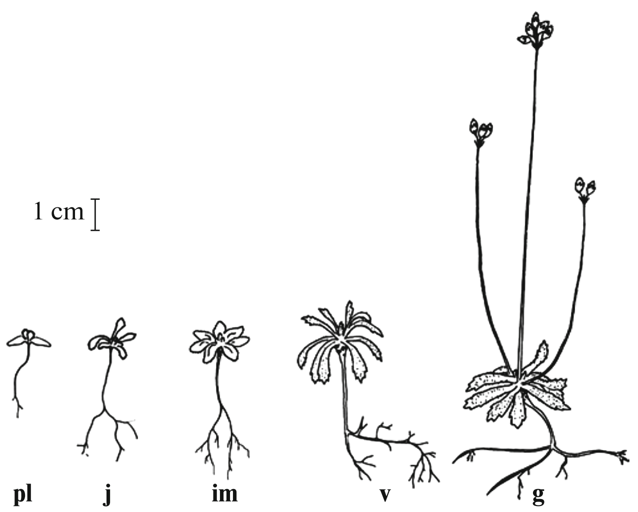

Fig. 1. Ontogenetic stages of *Androsace albana*: **pl**, plantules; **j**, juvenile plants; **im**, immature plants; **v**, adult vegetative plants, and **g**, generative plants.

with 1.5 cm in diameter, having 5–10 leaves. The leaves are oblong- or lanceolate-spatulate, with pointed apex, narrowed toward the base, sessile, the leaf margin being ciliated. The leaf length is 0.6 cm on average, the maximum width is above the leaf middle and averages 0.2 cm, the hypocotyl length is 8 mm. The main root, 1.5–2 cm long, begins to divaricate.

Immature plants. For the 2–3rd year of life, a shortened growth with 12–15 leaves develops from the apical bud of the main shoot. Leaves are oblong or lanceolate-spatulate with a pointed apex, narrowed toward the base, sessile, ciliated along the edge, assembled into a 2 cm diameter rosette. The leaf length is on average 1 cm, the maximum width is in the middle and averages 0.4 cm. The hypocotyl length is 8 mm. The main root with several second-order roots penetrates to a depth of 3 cm.

Adult virginal plants. For the 3–5th year of life, 16–30 leaves are formed from the apical bud of the main shoot. The leaves are sessile, drawn to the base, oblong or lanceolate-spatulate, with 4–7 obtuse denticles in the upper part. The leaves compose the rosette of 2–4.5 cm in diameter. The leaf length is 1.5–2 cm on average, the maximum width is in the middle and averages 0.5–0.7 cm. The upper surface and edge of the leaves are covered with cilia and dichotomously branching hairs, the lower surface being glabrate. The hypocotyl length is 0.9–2 cm, the width 1–2 mm. The length of the perennial shoot is 0.5–1 cm. Dead leaves of the last years remain on the perennial shoot for a long time. According to Popova's data (2010), the root system consists of a main root 5–6 cm long, of 3–5 second-order lateral roots, and a moderate number of fine roots of subsequent orders.

Generative plants. The first *A. albana* individuals flower on the 6th year. Generative shoots are leafless, 4 to 15 cm in height, 10 cm on average. The number of generative shoots varies from 1 to 8 on various individuals. Some of the leaves develop from the apical bud, the others from the axillary buds in the last year's growth of the main shoot. The leaves are morphologically similar to those of adult virgin plants. Generative shoots in the upper part are densely pubescent with simple and stellate hairs. The inflorescence of 2–15 almost sessile flowers are gathered into an almost capitate dense umbrella. The flowering period lasts from the end of June to the beginning of July. Seeds ripen by the end of August, pour out of the capsule in early September.

Senile plants. The senile period is not observed, the plants die off in the year of flowering.

Methods of Study

The research is carried out in the Karachay-Cherkess Republic, the territory of Teberda State Biosphere Reserve, on the Malaya Khatipara mountain, at the altitude of 2800 m asl.

In the first phase of research, we needed to determine the habitus of various stages in the ontogeny *A. albana*. With this purpose, in August 2009, we collected and alcoholized 10 to 20 individuals in each ontogenetic status (*Tsenopopulyatsii rastenii...*, 1976; *Sovremennye podhody...*, 2008). We used *Atlas on the Descriptive Morphology of Higher Plants: Leaf* (Fedorov et al., 1956, 1962; Artyushenko, 1990) as a reference to describe the stages of ontogeny based on the ontogeny periodization proposed by Rabotnov (1950a, 1950b).

In 2009, we laid down two transects of the 1.25 × 0.25 m size in the alpine lichen heaths, having five plots 0.25 × 0.25 m each. After the habitus of ontogenetic stages has been determined, all individuals of *A. albana* were put on the site plans with their own sequential numbers and marks of their ontogenetic stages. Next year, the individuals marked last year retain their last year's numbers, while the new ones acquired the new numbers; all individuals were classified by their ontogenetic stages at the time of observation. Monitoring was conducted in late August, each of the eight years from 2009 to 2016. This method enabled us to monitor the development of individual plants year by year over the total period of observation.

Life cycle graph (LCG), reflecting the biology of the species and the method of annual monitoring of the local population is shown in Fig. 2. Along with successive transitions from stage to stage in 1 year, there were also observed:

—delays ↪ in the **im** and **v** stages explainable by the fact that the harsh conditions of high mountains force plants to resort to the "space-holder strategy" strategy (Körner, 2003), which means to stay or grow in one place for as long as possible. Poor soils force some virginal plants to accumulate resources for fruiting for more than one year, the short growing season being a reason for some generative plants fail to realize their accumulated fruit-bearing potential (Rabotnov, 1946, 1949, 1950a; Harper and White, 1974; Körner, 2003; Bender et al., 2000; Keller and Vittoz, 2014);

—accelerated transitions **pl** ↝ **im** as a manifestation of the polyvariant ontogeny in *A. albana* under conditions of the alpine zone in the North-Western Caucasus.

There is only one reproductive event in the life span of each plant, but the population recruitment may be found in each of the three stages **pl**, **j** and **im** at the time of next census. Accordingly, parameters *a*, *b* and *c* have the meaning of the average (per one generative plant) number of recruiting individuals found in the corresponding stage at the next census.

Matrix model. In the matrix model, the population structure is described by the (column) vector $\boldsymbol{x}(t) = [pl(t), j(t), im(t), v(t), g(t)]^{\mathrm{T}}$, whose components are the numbers of individuals found in the corresponding stages of ontogeny in the year of observation *t*. How vector $\boldsymbol{x}(t)$ changes with years is described by the basic model equation of the vector-matrix form:

$$\boldsymbol{x}(t+1) = \boldsymbol{L}\boldsymbol{x}(t), t = 0, 1, \ldots, \tag{1}$$

where $\boldsymbol{L}$ is the *population projection matrix* (Caswell, 1989, 2001) associated with the LCG (Logofet and Belova, 2008) that is shown in Fig. 2, has the size 5 × 5 and the following pattern:

$$\boldsymbol{L} = \begin{bmatrix} 0 & 0 & 0 & 0 & a \\ d & 0 & 0 & 0 & b \\ e & f & h & 0 & c \\ 0 & 0 & k & l & 0 \\ 0 & 0 & 0 & m & 0 \end{bmatrix}; a, b, \ldots, l, m \geq 0. \tag{2}$$

The elements of matrix $\boldsymbol{L}$, or *vital rates*, *a*, *b*, ..., *l*, *m*, are subject to quantification (*calibration*) based on observational data.

The projection matrix is traditionally represented as the sum of two matrices:

$$\boldsymbol{L} = \boldsymbol{T} + \boldsymbol{F} = \begin{bmatrix} 0 & 0 & 0 & 0 & 0 \\ d & 0 & 0 & 0 & 0 \\ e & f & h & 0 & 0 \\ 0 & 0 & k & l & 0 \\ 0 & 0 & 0 & m & 0 \end{bmatrix} + \begin{bmatrix} 0 & 0 & 0 & 0 & a \\ 0 & 0 & 0 & 0 & b \\ 0 & 0 & 0 & 0 & c \\ 0 & 0 & 0 & 0 & 0 \\ 0 & 0 & 0 & 0 & 0 \end{bmatrix}, \tag{3}$$

where matrix $\boldsymbol{T}$ contains the parameters responsible for aging and ontogenetic transitions (*transition* matrix), and matrix $\boldsymbol{F}$ (*fertility* matrix) contains only the *reproduction rates* for the stage-classified groups (Cushing and Yicang, 1994; Caswell, 2001; Li and Schneider, 2002); all the other elements are zero in matrices $\boldsymbol{T}$ and $\boldsymbol{F}$.

Usually, the summands of sum (3) are calibrated differently due to the different meanings of their entries and to what is called "reproductive uncertainty" in data (Logofet, 2013a; Logofet et al., 2016, 2017c). However, in this case, the sole reproductive stage in the LCG eliminates any uncertainty as shown in the next section.

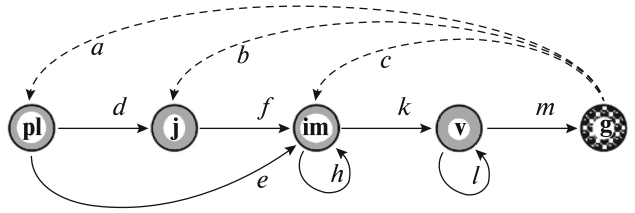

Fig. 2. Life cycle graph of *A. albana*: the same notations as in Fig. 1; dashed arrows indicate the recruitment found in the corresponding stages.

Calibration of matrices L. The type of data collected from the plots is known as "identifiable individuals" (Caswell, 2001, p. 134). The fate of each plant is tracked in consecutive censuses, which reduces the calibration of the matrix $\boldsymbol{T}$ in sum (3) to the direct calculation of its seven nonzero elements *d*, *e*, ..., *m* (Caswell, 2001; Logofet et al., 2017a, 2017b) in exact accordance with the demographic meaning of each of them as the fraction of those individuals of a certain stage group who, during the year since the previous census, have made the transition represented by the same-name arrow in Fig. 2. These fractions are different for the different years of observation, so that the calibrated matrices $\boldsymbol{T}(t)$ do differ and depend on the census year 2009, ..., 2015, or its ordinal number $t = 0, 1, \ldots, 6$. Formally, the model is therefore *nonautonomous*. To fix the ontogenetic transitions and population recruitment, the data of two consecutive censuses are needed, and therefore the number of calibrated matrices is always one less than the number of years of observations (8 years of observation provide for the calibration of 7 matrices).

Since only one reproductive event occurs in the *A. albana* life cycle, the elements of matrix $\boldsymbol{F}$, the reproduction rates *a*, *b*, *c* can also be calculated immediately from the data of two consecutive censuses as the average numbers (per one parent) of plantules, juvenile and immature plants, respectively, recruited to the population over the past year, i.e., from the moment *t* to $t + 1$. As a result, the time series of data of the "identified individuals" type over 8 years of observations provides for both the dynamics of the population structure $\boldsymbol{x}(t)$ and the 7 annual matrices $\boldsymbol{L}(t)$, which turn Eq. (1) into the 7 equalities that hold true according to the calibration conditions for $t = 0, 1, \ldots$. After that, the need and the opportunity arise to pose their averaging problem.

Averaging the annual projection matrices. In previous works (Logofet et al., 2107b, 2017c), it was shown that the correct mode of averaging several projection matrices is represented by the *geometric mean*. In our case, to get the population structure vector $\boldsymbol{x}(2016)$ observed in 2016 from the $\boldsymbol{x}(2009)$ vector observed in

2009, the initial vector should be multiplied sequentially by each of the calibrated annual matrices:

$$\boldsymbol{x}(2016) = \boldsymbol{L}_6 \cdot \boldsymbol{L}_5 \cdot \boldsymbol{L}_4 \cdot \boldsymbol{L}_3 \cdot \boldsymbol{L}_2 \cdot \boldsymbol{L}_1 \cdot \boldsymbol{L}_0 \cdot \boldsymbol{x}(2009). \qquad (4)$$

It means that a 7-time multiplication by the average geometric matrix $\boldsymbol{G}$ must give exactly the same result, i.e.

$$\boldsymbol{G}^7 = \boldsymbol{L}_6 \cdot \boldsymbol{L}_5 \cdot \boldsymbol{L}_4 \cdot \boldsymbol{L}_3 \cdot \boldsymbol{L}_2 \cdot \boldsymbol{L}_1 \cdot \boldsymbol{L}_0. \qquad (5)$$

The left- and right-hand sides of Eq. (5) represent matrices of 5 × 5 size. The *pattern* (i.e., the allocation of 15 zero and 10 nonzero elements) of the average matrix $\boldsymbol{G}$ ought to correspond the LCG (Fig. 2), i.e., this matrix of pattern (2) is defined by 10 positive elements a, b, ..., l, m, then raised to the 7th power. The expression on the right is the product of numerical matrices obtained as a result of model calibration, i.e., a matrix composed of 25 positive numbers. Written element-wise, the matrix Eq. (5) is essentially a system of 25 algebraic equations (one for each positive element of the product on the right-hand side) with respect to the 10 unknowns. Such systems are called *overdetermined*, and they have a solution only when the 15 redundant equations are some consequences of the 10 independent ones, i.e., they are automatically satisfied for the same values of unknowns as the 10 independent equations.

The formulation of the matrix model does not give any grounds for assuming a similar property in system (5), so that it does not have an exact solution in general. Therefore, the question whether of the geometric mean exists for several given non-negative (indecomposable) matrices is still open in matrix theory (Logofet, 2013b), and we only have to seek an approximate solution, i.e., a set of *feasible* values a, b, ..., l, m, which minimizes the *approximation error*, i.e., the deviation from zero in the left-hand side of the equation

$$\boldsymbol{G}^7 - \boldsymbol{L}_6 \cdot \boldsymbol{L}_5 \cdot \boldsymbol{L}_4 \cdot \boldsymbol{L}_3 \cdot \boldsymbol{L}_2 \cdot \boldsymbol{L}_1 \cdot \boldsymbol{L}_0 = \boldsymbol{0}. \qquad (6)$$

The constraints that determine the feasibility of a solution follow from the demographic meaning of the corresponding model parameters, and in addition, the idea of averaging implies that the elements of the average matrix should not leave the boundaries specified by the values of the corresponding elements in the matrices to be averaged. (Algebraic and technical details of the averaging problem are given in Appendix A.)

The location of the dominant eigenvalue $\lambda_1(\boldsymbol{G})$ of the average matrix $\boldsymbol{G}$ relative to 1 allows us to predict the population fate in the long-term perspective based on the eight years of observations: the growth, if $\lambda_1(\boldsymbol{G}) > 1$, decline if $\lambda_1(\boldsymbol{G}) < 1$, and stabilization if $\lambda_1(\boldsymbol{G}) = 1$.

Age-specific traits from the stage-structured model. Having the time step of 1 year, we can obtain certain *age* traits from the staged-structured model, guided by the following ideology (Cochran and Ellner, 1992; Bender et al., 2000; Caswell, 2011, Ch. 5). Note that matrix $\boldsymbol{T}$ in expression (3) is *substochastic* in columns, i.e., the sum of the elements in each of its columns does not exceed 1. This follows from the demographic meaning of each summand as the fraction of the groups of those individuals at the corresponding stage that have remained at this stage or moved to another one for the previous year; if the sum is less than one then the difference shows the proportion of dead individuals in this stage-specific group; if the sum is 1 then there have not been any perished ones. In the LCG (Fig. 2), matrix $\boldsymbol{T}$ is associated with the subgraph lacking arrows a, b, c.

Introduce an additional, the 6th in this case, state (**d**), which means the *death* of individuals. As a result, matrix $\boldsymbol{T}$ is supplemented with one more (the sixth in this case) row whose elements are the complements of the column sums to 1, and one more column with a single nonzero element corresponding to the eternal status of the state, $\mathbf{d} \curvearrowright \mathbf{d}$:

$$\left[\begin{array}{ccccc|c} 0 & 0 & 0 & 0 & 0 & 0 \\ d & 0 & 0 & 0 & 0 & 0 \\ e & f & h & 0 & 0 & 0 \\ 0 & 0 & k & l & 0 & 0 \\ 0 & 0 & 0 & m & 0 & 0 \\ \hline 1-d-e & 1-f & 1-h-k & 1-l-m & 1 & 1 \end{array}\right] = \boldsymbol{P}. \qquad (7)$$

Matrix $\boldsymbol{P}$ (4) is *substochastic* by constructon (all the column are 1), and this gives us grounds to consider it as the *transition probability matrix* of a discrete Markov chain: the states and probable transitions in this *virtual* chain are represented by the graph in Fig. 3a. Its subgraph without arrows ingoing to **d** coincides with the above-mentioned subgraph of the LCG (Fig. 2).

In Markov chain theory, the state **d** of the virtual chain is classified as *absorbing* (Kemeny and Snell, 1976, Ch. 3): once having reached it, the chain remains here forever. All other states are called *nonabsorbing*: the transitions between them are described by the principal submatrix $\boldsymbol{Q}$ of the transition matrix $\boldsymbol{P}$ constructed on the same columns and rows. The mathematical expectation of such a random variable as the number of steps that the chain sojourns in a given state before the moment of absorption is closely related to the *fundamental matrix* of the absorbing chain (Kemeny and Snell, 1976, Ch. 3),

$$\boldsymbol{N}[n_{ij}] = (\boldsymbol{I} - \boldsymbol{Q})^{-1}, \ \boldsymbol{I} = \operatorname{diag}\{1, \ldots, 1\}. \qquad (8)$$

Each of its elements, n_{ij}, is the average number of steps the transition process sojourns in the nonabsorbing state i before the moment of absorption if the initial state is j. Accordingly, the column sums of matrix $\boldsymbol{N}$ show the mean times spent in each of the nonabsorbing states, and these quantities are identified with the *life expectancy* (Caswell, 2001, p. 120) at the stage corresponding to the given column.

To calculate the mean age at the first (and the sole in *A. albana*) flowering, the “Markov superstructure” of the model must be different. Essentially, we are talking about the age of reaching stage **g**, and there is no need to introduce an additional absorbing state "survive to reproduction" as in polycarpic species (Logofet et al., 2017c). Clearly, this trait is relevant to only those plants that have reached the generative stage one way or another in their development, and therefore the digraph of the virtual chain looks as shown in Fig. 3b. The conditional transition probabilities d^c, e^c, ..., l^c, m^c are the elements of the transition matrix

$$\boldsymbol{P}^c = \left[\begin{array}{cccc|c} 0 & 0 & 0 & 0 & 0 \\ d^c & 0 & 0 & 0 & 0 \\ e^c & f^c & h^c & 0 & 0 \\ 0 & 0 & k^c & l^c & 0 \\ \hline 0 & 0 & 0 & m^c & 1 \end{array}\right], \tag{9}$$

to be recalculated from the elements d, e, ..., l, m of the average matrix $\boldsymbol{G}$ under the condition of no death (Appendix B). In this case, submatrix $\boldsymbol{Q}$ is the principal 4 × 4 submatrix of matrix $\boldsymbol{P}^c$ (9), and still the column sums of the fundamental matrix (8) give the status-specific age traits, and the unknown age of flowering is the expected number of years that plantules spend in all stages until the final one is reached, i.e., it equals the sum of the first column in matrix (8).

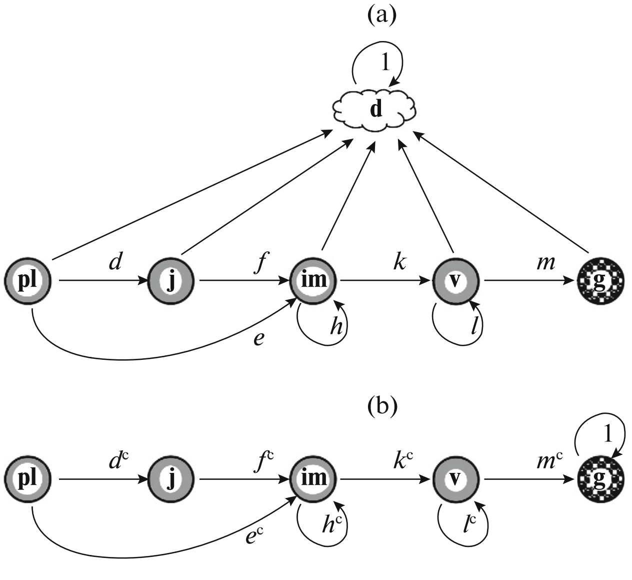

Fig. 3. Digraphs of the virtual Markov chain for calculating: (a) the life expectancy; (b) the mean age of flowering.

RESULTS

Local Population Structure and Dynamics

Changes in the sizes of stage groups by year are presented in Table 1. The local population of *A. albana* is a normal *complete* population, i.e., it contains individuals of all stage statuses, with the left-side type of "age spectrum" in the Uranov's (1975) terminology.

The number of plantules on the plots under study varies from 4 to 49 plants, of juvenile plants from 29 to 110, immature ones from 13 to 99 from, adult virgins from 16 to 73 from, and generative plants from 1 to 13 from (Table 1). On average, for 8 years of observation: 49% of the populations are shared by plantules and juveniles, the same share by immature and adult virginal plants, and only 2% by generative ones.

Calibrated Matrices L(t)

Table 2 helps calculating the elements of projection matrices as there are all the recruitment individuals and all the transitions between the stages counted. The elements of the annual matrices $\boldsymbol{L}(t)$ (Table 3) are obtained from the corresponding cells of Table 2 via dividing by the size of the group. Variation in matrices with years are quite significant, with the 4 out of 7 matrices giving a measure of adaptation $\lambda_1(\boldsymbol{L})$ much less than 1, which indicates a depressed status of the local population.

Geometric Mean of the Annual Matrices

As noted above, there is no exact solution of the averaging problem in this case, and the approximate solution for the seven matrices in Table 3, with a rather high accuracy of approximation (Appendix A), is given by the matrix shown in Table 4. Its pattern obviously corresponds to the LCG (Fig. 2), and the values of the transition and reproduction rates do not leave the boundaries specified by the corresponding elements of the matrices to be averaged (Table 3). In the transitional part $\boldsymbol{T}$ of the matrix $\boldsymbol{G}$, a tendency has clearly manifested that occurred only for some annual matrices $\boldsymbol{T}(t)$: the positive elements decrease with the row number in each column. In a *unidirectional* (i.e., without returns) process (Fig. 2), this means that plants are more often delayed in development than they transit to the next stage, and the accelerated transitions (skipping a stage) are less likely than successive ones.

Despite the values of $\lambda_1(t) > 1$ for $t = 2010–2012$, the trend towards decrease does predominate in the local population over the 8-year observation period, which is expressed by the value of $\lambda_1(\boldsymbol{G}) < 1$ (Table 4). The shape of the *equilibrium structure* (of the normalized dominant eigenvector $\boldsymbol{x}^*$) is rather two-humped than left-sided, with the maxima at the juvenile and virgin stages (Table 4). So, it is essentially different from the structure of the local population obtained by arithmetic averaging (Table 1), adding one more argument against the arithmetic mean in matrix models.

Life Expectancy

The age traits calculated by formula (6) for the averaged model are presented in Table 5 (with an accuracy up to the 4th decimal place for the original

Table 1. Structure of the local *A. albana* by years according to observation data

Stage	Stage group size at the year of observation								Average, %
	2009	2010	2011	2012	2013	2014	2015	2016	
pl	37	30	19	49	19	16	4	10	12
j	110	48	45	86	137	98	19	29	37
im	99	55	43	87	95	34	10	13	28
v	35	26	57	58	73	50	20	16	21
g	13	1	1	4	6	3	4	2	2

Table 2. Towards calculating the model parameters: the number of the recruiting plants and the transitions along the arcs of LCG (Fig. 2) in accordance with census data

Transition	Census year (time *t* + 1)						
	2010	2011	2012	2013	2014	2015	2016
a: **pl** ↷ **g**	30	19	49	19	16	4	10
b: **j** ↷ **g**	40	31	85	136	98	19	29
c: **im** ↷ **g**	3	0	25	1	2	0	7
d: **pl** → **j**	8	14	1	1	0	0	0
e: **pl** ⤻ **im**	2	4	6	10	2	2	0
f: **j** ⟲ **j**	22	22	35	45	16	2	3
h: **im** ⟲ **im**	28	17	21	39	14	6	3
k: **im** → **v**	7	34	10	28	6	4	2
l: **v** ⟲ **v**	19	23	48	45	44	16	14
m: **v** → **g**	1	1	4	6	3	4	2

submatrix $\boldsymbol{Q}$ and up to the third decimal place for the fundamental matrix $\boldsymbol{N} = [n_{ij}]$).

The decrease of the positive elements n_{ij} with increasing row numbers in each column reflects the above-mentioned tendency in the development of *A. albana* and, according to the meaning of the elements, shows that the life expectancy at each stage is distributed among subsequent stages in favor of a longer stay in the earlier stages. Life expectancy is logically equal to 1 in generative plants as their ages end in the same season (Fig. 3a, matrix (7)). The greatest (4 years) value of stage **v** (in adult virgin plants) is due to the highest value of the delay probability at this stage (element (4, 4) of matrix $\boldsymbol{G}$, Table 4). Long stay in the vegetative phase is an adaptive feature of plants growing in cold biomes (Nakhutsrishvili and Gamtsemlidze, 1984; Pavlov and Onipchenko, 1987) and a sign of the *space holder* strategy by Körner (2003) or the *delayed-development* strategy by Zhukova (1995). *A. albana* shows commitment to this strategy during the total 8-year observation period.

Mean age at first flowering is one of the four stage-specific traits, $A_{\mathbf{s}}$, meaning the average number of steps needed for the individual at stage **s** (**s** = **pl**, **j**, **im**, **v**) to reach the flowering stage **g**, namely, $A_{\mathbf{pl}} = 13.5$ years (Table 5). Paradoxically, at first glance, it exceeds the life expectancy of individuals at every stage. The paradox is resolved by the fact the life expectancy does account for the death probability at each of the stages (which is maximal in juveniles, see the 2nd column of matrix $\boldsymbol{G}$, Table 4), whereas the age of flowering is determined only among the plants that survived flowering. It may also seem alarming that 13.5 years is beyond the time horizon of observations (8 years). However, there is no contradiction with the field data, where the plants were found not younger than 8 years old, but not yet reached the generative stage.

DISCUSSION

In the national studies, the history of using the technique of virtual absorbing Markov chains to estimate the age traits (in years) in local populations is reduced to a small number of examples focused on alpine herbaceous perennial (or shirt-lived perennial) species. Without any explicit slogan of "age-specific

Table 3. The outcome of matrix (2) calibration for *A. albana* according to the data of Tables 1, 2

Census year	Matrix $\boldsymbol{L}(t)$	$\lambda_1(\boldsymbol{L}(t))$	Vector $\boldsymbol{x}^*$, %	$\Delta\left(\frac{x(t)}{\|x(t)\|_1} - x^*\right)$
2009 $t = 0$	$\begin{bmatrix} 0 & 0 & 0 & 0 & 30/13 \\ 8/37 & 0 & 0 & 0 & 40/13 \\ 2/37 & 22/110 & 28/99 & 0 & 3/13 \\ 0 & 0 & 7/99 & 19/37 & 0 \\ 0 & 0 & 0 & 1/35 & 0 \end{bmatrix}$	0.5661	$\begin{bmatrix} 10.61 \\ 18.20 \\ 16.99 \\ 51.59 \\ 2.60 \end{bmatrix}$	39.68
2010 $t = 1$	$\begin{bmatrix} 0 & 0 & 0 & 0 & 19/1 \\ 14/30 & 0 & 0 & 0 & 31/1 \\ 4/30 & 22/48 & 17/55 & 0 & 0/1 \\ 0 & 0 & 34/55 & 23/26 & 0 \\ 0 & 0 & 0 & 1/26 & 0 \end{bmatrix}$	1.2283	$\begin{bmatrix} 15.90 \\ 31.99 \\ 18.25 \\ 32.83 \\ 1.03 \end{bmatrix}$	18.97
2011 $t = 2$	$\begin{bmatrix} 0 & 0 & 0 & 0 & 49/1 \\ 1/19 & 0 & 0 & 0 & 85/1 \\ 6/19 & 35/45 & 21/43 & 0 & 25/1 \\ 0 & 0 & 10/43 & 48/57 & 0 \\ 0 & 0 & 0 & 4/57 & 0 \end{bmatrix}$	1.5779	$\begin{bmatrix} 17.20 \\ 30.40 \\ 39.39 \\ 12.45 \\ 0.55 \end{bmatrix}$	22.15
2012 $t = 3$	$\begin{bmatrix} 0 & 0 & 0 & 0 & 19/4 \\ 1/49 & 0 & 0 & 0 & 136/4 \\ 10/49 & 46/86 & 39/87 & 0 & 1/4 \\ 0 & 0 & 28/87 & 45/58 & 0 \\ 0 & 0 & 0 & 6/58 & 0 \end{bmatrix}$	1.2641	$\begin{bmatrix} 6.01 \\ 43.15 \\ 29.67 \\ 19.56 \\ 1.60 \end{bmatrix}$	13.06
2013 $t = 4$	$\begin{bmatrix} 0 & 0 & 0 & 0 & 16/6 \\ 0 & 0 & 0 & 0 & 98/6 \\ 2/19 & 16/137 & 14/95 & 0 & 2/6 \\ 0 & 0 & 6/95 & 44/73 & 0 \\ 0 & 0 & 0 & 3/73 & 0 \end{bmatrix}$	0.6345	$\begin{bmatrix} 7.76 \\ 47.54 \\ 14.34 \\ 28.51 \\ 1.85 \end{bmatrix}$	14.45
2014 $t = 5$	$\begin{bmatrix} 0 & 0 & 0 & 0 & 4/3 \\ 0 & 0 & 0 & 0 & 19/3 \\ 2/16 & 2/98 & 6/34 & 0 & 0/3 \\ 0 & 0 & 4/34 & 16/50 & 0 \\ 0 & 0 & 0 & 4/50 & 0 \end{bmatrix}$	0.3988	$\begin{bmatrix} 1.71 \\ 56.64 \\ 11.69 \\ 17.46 \\ 3.50 \end{bmatrix}$	12.64
2015 $t = 6$	$\begin{bmatrix} 0 & 0 & 0 & 0 & 10/4 \\ 0 & 0 & 0 & 0 & 29/4 \\ 0 & 3/19 & 3/10 & 0 & 7/4 \\ 0 & 0 & 2/10 & 14/20 & 0 \\ 0 & 0 & 0 & 2/20 & 0 \end{bmatrix}$	0.8382	$\begin{bmatrix} 11.13 \\ 32.27 \\ 21.60 \\ 31.27 \\ 3.73 \end{bmatrix}$	8.17

traits from state-structured models" (Caswell, 2001, p. 116), yet by means of the fundamental matrix of the virtual chain, the first attempt in Russia to estimate the average duration of ontogenetic stages was undertaken by Sizov et al. (1999) in the framework of matrix population models for the dynamics of perennial herbaceous species with polyvariant ontogeny, but those works have not been further developed. The technique is applied to the transition part $\boldsymbol{T}$ of the projection matrix $\boldsymbol{L} = \boldsymbol{T} + \boldsymbol{F}$, hence it gives unambiguous results even in the case of data with reproductive uncertainty (Logofet et al., 2017b, 2017c). In combination with the

Table 4. Geometric mean, $\boldsymbol{G}$, of the annual matrices $\boldsymbol{L}(t)$

Matrix $\boldsymbol{G}$	$\lambda_1(\boldsymbol{G})$	Equilibrium structure, %	Stage
$\begin{bmatrix} 0 & 0 & 0 & 0 & 3.9457 \\ 0.4667 & 0 & 0 & 0 & 9.3226 \\ 0.1053 & 0.1946 & 0.3197 & 0 & 0.2308 \\ 0 & 0 & 0.1230 & 0.7299 & 0 \\ 0 & 0 & 0 & 0.1034 & 0 \end{bmatrix}$	0.832183	13.8 40.4 19.5 23.4 2.9	**pl** **j** **im** **v** **g**

Table 5. Age-specific traits of *A. albana* as a result of averaging the annual matrices $\boldsymbol{T}(t)$

Trait	Submatrix $\boldsymbol{Q}$	Fundamental matrix, $\boldsymbol{N} = (\boldsymbol{I} - \boldsymbol{Q})^{-1}$	Stage-specific values (years) ± standard deviation				
			pl	**j**	**im**	**v**	**g**
E_s	$\begin{bmatrix} 0 & 0 & 0 & 0 & 0 \\ 0.4667 & 0 & 0 & 0 & 0 \\ 0.1053 & 0.1946 & 0.3197 & 0 & 0 \\ 0 & 0 & 0.1230 & 0.7299 & 0 \\ 0 & 0 & 0 & 0.1034 & 0 \end{bmatrix}$	$\begin{bmatrix} 1 & 0 & 0 & 0 & 0 \\ 0.467 & 1 & 0 & 0 & 0 \\ 0.288 & 0.286 & 1.470 & 0 & 0 \\ 0.131 & 0.130 & 0.669 & 3.703 & 0 \\ 0.014 & 0.013 & 0.069 & 0.383 & 1 \end{bmatrix}$	1.90 1.41	1.43 1.32	2.21 2.24	4.01 3.20	1.00 0
A_s	$\begin{bmatrix} 0 & 0 & 0 & 0 \\ 0.8160 & 0 & 0 & 0 \\ 0.1840 & 1 & 0.7222 & 0 \\ 0 & 0 & 0.2778 & 0.8759 \end{bmatrix}$	$\begin{bmatrix} 1 & 0 & 0 & 0 \\ 0.816 & 1 & 0 & 0 \\ 3.600 & 3.600 & 3.600 & 0 \\ 8.056 & 8.056 & 8.056 & 8.056 \end{bmatrix}$	13.47 8.15	12.66 8.14	11.66 8.14	8.06 7.54	

E_s is the life expectancy at stage; **s** (**s** = **pl**, **j**, **im**, **v**, **g**); A_s is the average number of steps before reaching the generative stage from stage; **s** (**s** = **pl**, **j**, **im**, **v**); A_{pl} is the mean age at flowering.

geometric averaging of a set of annual projection matrices (Logofet et al., 2017b, 2017c), it enables us to derive the indices characterizing the local population over the whole period of observations, and for the age at first flowering it gives the values that go beyond the horizon of the time series (Table 5; Logofet et al., 2017c, Table 2). Direct records of the number of years between germination and the first flowering required much longer observations (Kipkeev et al., 2015).

When calibrated from the observation data, the annual matrices $\boldsymbol{L}(t)$ (Table 3) represent an objective, yet indirect, picture variations in those environmental conditions to which the local population is sensitive, and this picture convinces that the conditions were very crucial: the measure of fitness $\lambda_1(\boldsymbol{L}(t))$ falls to extremely low values for some years, e.g., below 0.4 in the interval between the 2014–2015 censuses, and the recruitment in 2015 was the smallest in all three stages for the entire observation period (Table 1). Within that interval, the conditions for young *A. albana* plants (plantules, juvenile, immature) surviving, for adults (vegetative and generative) overwintering and growth were likely to be the most severe of the entire observation period. Were they repeated for at least 2 successive years, the local population would be reduced to less than $0.4^2 \times 100\% = 16\%$ of its size, for 3 successive years, then to $0.4^3 \times 100\% \approx 6\%$. The extinction danger is also confirmed by the less-than-1 dominant eigenvalue $\lambda_1(\boldsymbol{G})$ of the matrix $\boldsymbol{G}$ averaged over the whole period of observations (Table 4). An even smaller value (0.7792) is yielded by the 7th power root of the dominant eigenvalue that the product of seven matrices $\boldsymbol{L}(t)$ from Table 3 does yield. This value shows the asymptotic (long-term) growth rate of the local population at a strictly periodic, with a period of 7 years, sequence of matrices $\boldsymbol{L}(t)$, i.e., with repeating periodically the conditions of the observation period.

There are several reasons for reducing the adaptation of *A. albana* in this habitat. For example, the role of seed is extremely high in the lifespan of flowering plants, and the seed is an indispensable link in the train of generations (Markov, 2012). Therefore, the authors, in addition to observing the marked individuals, conducted a research on the parameters of seed renewal in *A. albana*. As a result, it was found that the seed production is low in this species and amounts to 47 ± 6 seeds per generative shoot, the seed mass being moderate (0.7 mg), the germination being moderate too (19–48%); the first plantules appear late, on the 12th and 22nd day of the experiment (Kazantseva et al., 2016). The small number of plantules in the *A. albana* population may be due to both weather conditions (Onipchenko and Komarov, 1997), and a small size of the seedbank in this species (Semenova and Onipchenko, 1996). However, even after a year of small recruitment, the number of vegetative plants did practically not decrease for the subsequent year. Similar effects were observed in other studies of alpine plant communities (Diemer, 1992; Körner, 2003), where a significant changes from year to year in the share of plantules did not significantly correlate with those in the composition of the adult population. The latter means that the viabilities of plantules and adults are determined by different factors, and this helps the population to survive in extreme conditions of high mountains.

The low seed production in *A. albana* might also be a reason for the low number of plantules, while severe weather and habitat conditions be a reason for their deaths. These have led to the inclusion of this species into the *The Red Data Book of the Krasnodar Krai* (*Krasnaya kniga Krasnodarskogo...*, 2007) and *The Red Data Book of the Adygea Republic* (*Krasnaya kniga Respubliki Adygeya...*, 2012).

Parameters of the leaf apparatus in *A. albana* (Shidakov and Onipchenko, 2007) indicate the adherence of this species to SR-strategies (Kazantseva, 2016; Pierce et al., 2017), i.e., the plants exist due to their endurance, can grow in extremely harsh habitats, are well adapted to the temporal pulsation of the resource availability (Grime, 1979, 2001; Onipchenko, 2013). The local population of *A. albana* does survive due to the persistence of adult virgin individuals and the high growth potential in favorable years (2010–2012, Table 3). For this reason, *A. albana*, though rare, can be found in the Teberdinsky Reserve, in the lichen heaths on rocky places and screes in the alpine belt, at the altitude of 2400–2850 m (Vorob'yova and Onipchenko, 2001), and it tends toward communities with low closeness in the grass and dwarf shrub layers (Egorov et al., 2012).

Noted in the Results, the "left-handed age spectrum" effect in the local population of *A. albana* was not observed in all the years excepting 2010–2012 (Table 1), and it was these years for which the fitness measure $\lambda_1(\boldsymbol{L}(t))$, the growth potential of the population, has been noticeably more than 1 (Table 3). But the left-side spectrum feature is traditionally associated with growing populations, which contradicts the situation we observe. The contradiction is explained by the fact that the above comparison with the "left-sided age spectrum" is only a tribute to the persistent tradition of the national school of plant ecology, but it is hardly appropriate to the stage-structured model where individuals of different chronological ages can occur at all stages beginning with the immature one.

In some alpine species with longer life cycles, for example, in *Anemona speciosa* (Onipchenko and Komarov, 1997), the maximum of the "age spectrum" shifted to the adult virginal stage, but the number of generative *A. speciosa* plants was also relatively high in contrast to our observations. However, *A. speciosa* is not included into the *Red Books of the Caucasus*, so the "two-humped" equilibrium population structure in the averaged model (Table 4) may serve as another indicator of a declining population.

It is methodologically interesting to compare the solution of the averaging problem for projection matrices $\boldsymbol{L}(t)$ found here by the direct method, and that by the "heuristic" method proposed by Logofet et al. (2017c) for the case of data with "reproductive uncertainty." In this case, only the transition part $\boldsymbol{T}(t) = \boldsymbol{L}(t) - \boldsymbol{F}(t)$ of annual matrices is uniquely calculated in the calibration, while the status-specific reproduction rates, the elements of matrix $\boldsymbol{F}(t)$, get only certain ranges for the variations that are compatible with the census data (Logofet et al., 2017c). Then the averaging problem is solved in a combined way: we find the best approximation for the geometric mean of the annual matrices $\boldsymbol{T}(t)$, and we average the matrices $\boldsymbol{F}(t)$ by the methods of interval arithmetic ($\boldsymbol{F}(t)$ reduces simply to the arithmetic mean (Appendix B). In this case, the approximation error of the geometric mean decreases by more than 2 orders of magnitude (due to the substochasticity of $\boldsymbol{T}$), but the dominant eigenvalue of the combined average $\boldsymbol{L}_{\mathbf{cmb}}$ is essentially overestimated:

$$l_1(\boldsymbol{L}_{\mathbf{cmb}}) = 1.05196\ldots > 1, \qquad (10)$$

where is the value $\lambda_1(\boldsymbol{G})$ locates to the left of 1 (Table 4), indicating the population decline in the long-term perspective. The inflated results of arithmetic averaging as compared to geometric averaging have deep roots in the elementary algebraic inequality $(a + b)/2 \geq \sqrt{ab}$, which is true for any positive numbers a, b, and example (10) shows that the forecasts based on combined averaging should be treated with caution.

CONCLUSIONS

The "scale of ontogenesis" and the LCG of *A. albana* plants are constructed by the results of 8-year observations on permanent plots in the alpine lichen heath. The LCG reflects the unidirectional development of individuals in a monocarpic species and serves as a basis for constructing a matrix model of stage-structured population dynamics. The type of data and the sole reproductive event in the lifespan enable calibration of the model in a unique way by the data of two consecutive censuses (i.e., on one time step), which results in the model becoming *nonautonomous*, with seven annual matrices $\boldsymbol{L}(t)$. Each of them fixes the environmental conditions on its own time step, and they demonstrate significant variations in the value of $\lambda_1(\boldsymbol{L}(t))$, the measure of adaptation to the environment in the time period $[t, t + 1]$, i.e., a high level of population vulnerability to environmental stresses. Averaging the matrices over the entire time series of observations gives the value of $\lambda_1 \approx 0.83$, i.e., it predicts the extinction of the local population if the conditions realized in the observation period remain the same for a long time. This is also evidenced by the 13 years as the mean (over the local population) age of flowering, which reduces the reproduction rates and increases the risk of plants dying at early ages. Therefore, the life expectancy of plantules is only 2 years in this short-lived perennial species and only 4 years in the adult plants.

APPENDIX A

The Problem to Average the Population Projection Matrices

The geometric mean of the seven projection matrices $\boldsymbol{L}(t)$ presented in Table 3 is the best approximate solution to the matrix Eq. (6), i.e., such a set of 10 positive parameters *a, b, ..., l, m* that delivers the minimum to the quadratic sum of deviations from zero over all the 10 nontrivial elements of the matrix difference on the left-hand side of Eq. (6), or, in formal terms,

$$\min_{\mathbb{B}} \left\| \begin{bmatrix} 0 & 0 & 0 & 0 & a \\ d & 0 & 0 & 0 & b \\ e & f & h & 0 & c \\ 0 & 0 & k & l & c \\ 0 & 0 & 0 & m & 0 \end{bmatrix}^7 - [\boldsymbol{L}_6 \cdot \boldsymbol{L}_5 \cdot \boldsymbol{L}_4 \cdot \boldsymbol{L}_3 \cdot \boldsymbol{L}_2 \cdot \boldsymbol{L}_1 \cdot \boldsymbol{L}_0] \right\|. \qquad \text{(A1)}$$

Here ‖ ... ‖ denotes the Euclidean norm, while the exact form of the product $\boldsymbol{L}_6 \cdot \boldsymbol{L}_5 \cdot \boldsymbol{L}_4 \cdot \boldsymbol{L}_3 \cdot \boldsymbol{L}_2 \cdot \boldsymbol{L}_1 \cdot \boldsymbol{L}_0$ obtained with machine symbolic algebra is too cumbersome for publication.

In the *constraint minimization* problem (A1), the above parameters *a, ..., m* represent *variables*, whose set of feasible values, $\mathbb{B}$, is a parallelepiped in $\mathbb{R}_+^{10}$ obtained from the following considerations. Since being elements of the average matrix, the parameters $[a, ..., m] = \boldsymbol{g} \in \mathbb{R}_+^{10}$ should not leave the ranges of their values in the matrices $\boldsymbol{L}_t$ $(t = 0, 1, ..., 6)$ to be averaged. Thus, we have

$$\min \boldsymbol{L} \le \boldsymbol{g} \le \min \boldsymbol{L}, \qquad \text{(A2)}$$

where the vectors min$\boldsymbol{L}$ and max$\boldsymbol{L}$ are composed of the corresponding nonzero elements of matrices $\boldsymbol{L}_t$:

$$\begin{aligned} \min \boldsymbol{L} &= .\min{}^{+}\{\boldsymbol{L}_0, \boldsymbol{L}_1, \ldots, \boldsymbol{L}_6\}, \\ \max \boldsymbol{L} &= .\max{}^{+}\{\boldsymbol{L}_0, \boldsymbol{L}_1, \ldots, \boldsymbol{L}_6\}, \end{aligned} \qquad \text{(A3)}$$

and the dot before the function name means its element-wise execution. Function $\min^+$ chooses the minimal number out of the given positive ones, i.e., it eliminates 0 from the outcome:

$$\min{}^{+}(x, y) = \begin{cases} \min(x, y), \text{ if } x \cdot y \ne 0, \\ \max(x, y), \text{ if } x \cdot y = 0, \end{cases} \qquad \text{(A4)}$$

Otherwise, the optimization might have attained a zero value of an entry to $\boldsymbol{G}$, hence the corresponding arc would have disappeared from the LCG.

Strictly speaking, we had to carve a polyhedron from the parallelepiped $\mathbb{B}$ by the conditions of the transition part $\boldsymbol{T} = \boldsymbol{G} - \boldsymbol{F}$ being substochastic along those columns where there are more than one elements, i.e., by

$$d + e \le 1, \quad h + k \le 1, \quad l + m \le 1, \qquad \text{(A5)}$$

(the constraints on single elements follow automatically from (A2)). However, it is technically simpler to verify $\boldsymbol{T}$being substochastic just in the optimal solution obtained for $\mathbb{B}$.

We retrieve a solution to the problem (A1)–(A3) using the library function *fmincon*(...) in the Matlab environment (MathWorks, 2016), the norm of difference in expression (A1) using a special, user-defined function *normG7_prodL*($\boldsymbol{g}$) of the vector argument $\boldsymbol{g} \in \mathbb{R}_+^{10}$, while the upper and lower bounds of variables are given by conditions (A2). The following Matlab string:

$$\begin{aligned} \gg [\boldsymbol{g},\ FVAL] = fmincon(@normG7\_prodL, \\ \boldsymbol{g0}, [\ ], [\ ], [\ ], [\ ],\ \min \boldsymbol{L},\ \max \boldsymbol{L}), \end{aligned} \qquad \text{(A6)}$$

launches the optimization procedure after the technical parameters of optimization have been properly adjusted (MathWorks, 2016); notation "[], []," means the lack of equality constraints and nontrivial inequalities of (A5) type in the problem formulation, vector $\boldsymbol{g0} \in \mathbb{R}_+^{10}$ is the starting point for the algorithm searching for a solution, the output argument (in the left-hand side of (A6)) $\boldsymbol{g} \in \mathbb{R}_+^{10}$ is the (local) solution found, *FVAL* is the minimal value it delivers to function *normG7_prodT*.

A diverse (randomly generated) choice of the initial vector $\boldsymbol{g0}$ yielded different local solutions $\boldsymbol{g}$, the difference in the approximation quality (in the *FVAL* values) reaching two orders of magnitude. Close to the global minimum, the value of *FVAL* = 2.2297455...× 10^{-2} is attained for $\boldsymbol{g0} = [1 \ldots 1]/10$, after which the repeated starts of the SQR algorithm right from the found solution **g** improves *FVAL* up to 2.2297455...× 10^{-2}, the global minimum achievable at

$$\boldsymbol{G}_{\text{opt}} = \begin{bmatrix} 0 & 0 & 0 & 0 & 3.945665 \\ 0.466667 & 0 & 0 & 0 & 9.322562 \\ 0.105263 & 0.194595 & 0.319716 & 0 & 0.230769 \\ 0 & 0 & 0.122988 & 0.729939 & 0 \\ 0 & 0 & 0 & 0.103448 & 0 \end{bmatrix} \qquad \text{(A7)}$$

(with an accuracy of 10^{-6}).

Substochasticity constraints are obviously met; to see which of the given faces of $\mathbb{B}$ are attained in the optimal solution with an accuracy, e.g., to 10^{-6}, we perform the following Matlab-command of the logical comparison:

$$\gg \mathrm{round}(10\mathrm{e}+6{*}\boldsymbol{g}) = \mathrm{round}(10\mathrm{e}+6{*}\min \boldsymbol{L}),$$

which returns

$$\mathrm{ans} = 0010100000.$$

This means that the lower faces are attained by parameters c and e. Similarly, the upper faces are revealed by the Matlab command

$$\gg \mathrm{round}(10\mathrm{e}+6{*}\boldsymbol{g}) = \mathrm{round}(10\mathrm{e}+6{*}\max \boldsymbol{L}),$$

which returns

$$\mathrm{ans} = 0001000001.$$

meaning that the upper bounds are attained by d and m.

APPENDIX B

Transition Matrix of the Conditional Chain for Calculating the Mean Age of Flowering

According to the digraph of the virtual absorbing Markov chain (Fig. 3b), the transition matrix of the chain has pattern (9) and, after recalculating its elements from the matrix $\boldsymbol{T}(3)$, takes on the form:

$$\boldsymbol{P}^{\mathrm{c}} = \left[\begin{array}{cccc|c} 0 & 0 & 0 & 0 & 0 \\ d^{\mathrm{c}} & 0 & 0 & 0 & 0 \\ e^{\mathrm{c}} & f^{\mathrm{c}} & h^{\mathrm{c}} & 0 & 0 \\ 0 & 0 & k^{\mathrm{c}} & l^{\mathrm{c}} & 0 \\ \hline 0 & 0 & 0 & m^{\mathrm{c}} & 1 \end{array}\right] = \left[\begin{array}{cccc|c} 0 & 0 & 0 & 0 & 0 \\ d/(d+e) & 0 & 0 & 0 & 0 \\ e/(d+e) & 1 & h/(h+k) & 0 & 0 \\ 0 & 0 & k/(h+k) & l/(l+m) & 0 \\ \hline 0 & 0 & 0 & m/(l+m) & 1 \end{array}\right]. \tag{B1}$$

The column stochastic property is obvious in (B1). If we denote the outlined principal 4 × 4 submatrix as $\boldsymbol{Q}_{\mathbf{af}}$, the following Matlab string:

$$\gg \mathrm{Naf} = \mathrm{inv}(\mathrm{eye}(4) - \mathrm{Qaf}),$$

returns the fundamental matrix $\boldsymbol{N}_{\mathbf{af}}$:

$$\mathrm{Naff} = \begin{array}{llll} [1 & 0 & 0 & 0] \\ [\mathrm{d}/(\mathrm{d}+\mathrm{e}) & 1 & 0 & 0] \\ [(\mathrm{h}+\mathrm{k})/\mathrm{k} & (\mathrm{h}+\mathrm{k})/\mathrm{k} & (\mathrm{h}+\mathrm{k})/\mathrm{k} & 0] \\ [(1+\mathrm{m})/\mathrm{m} & (1+\mathrm{m})/\mathrm{m} & (1+\mathrm{m})/\mathrm{m} & (1+\mathrm{m})/\mathrm{m}] \end{array}.$$

APPENDIX C

"Combined" Averaging Problem for Projection Matrices

The combined averaging of annual projection matrices $\boldsymbol{L}(t) = \boldsymbol{T}(t) + \boldsymbol{F}(t)$, $t = 0, 1, \ldots, 6$ (Table 3) reduces to finding the approximate geometric mean, $\boldsymbol{T}_{\mathbf{gm}}$, of matrices $\boldsymbol{T}(t)$ and the arithmetic mean $\boldsymbol{F}_{\mathbf{am}}$, of matrices $\boldsymbol{F}(t)$, thereby we calculate the combined average, $\boldsymbol{L}_{\mathbf{cmb}}$, of the annual matrices $\boldsymbol{L}(t)$ as

$$\boldsymbol{L}_{\mathbf{cmb}} = \boldsymbol{T}_{\mathbf{gm}} + \boldsymbol{F}_{\mathbf{am}} = \begin{bmatrix} 0 & 0 & 0 & 0 & 0 \\ d & 0 & 0 & 0 & 0 \\ e & f & h & 0 & 0 \\ 0 & 0 & k & l & 0 \\ 0 & 0 & 0 & m & 0 \end{bmatrix} + \begin{bmatrix} 0 & 0 & 0 & 0 & a \\ 0 & 0 & 0 & 0 & b \\ 0 & 0 & 0 & 0 & c \\ 0 & 0 & 0 & 0 & 0 \\ 0 & 0 & 0 & 0 & 0 \end{bmatrix}. \tag{C1}$$

Matrix $\boldsymbol{T}_{\mathbf{gm}}$ is obtained from the solution of the constraint minimization problem, in which the variables $[d, \ldots, m] = \boldsymbol{gT} \in \mathbb{R}_+^7$ are bounded from below and above similarly to condition (A2):

$$\min\boldsymbol{T} \le \boldsymbol{gT} \le \max\boldsymbol{T}, \tag{C2}$$

where min$\boldsymbol{T}$ and max$\boldsymbol{T}$ are vectors composed of the corresponding nonzero elements of matrices $\boldsymbol{T}_t$. The Matlab string similar to (A6):

$$\gg [\boldsymbol{gT},\ FVAL] = fmincon(@\,normT7\_prodT,\ \boldsymbol{gT0},\ [\ ],[\ ],[\ ],[\ ],\ \min\boldsymbol{T},\ \max\boldsymbol{T}), \tag{C3}$$

launches the constraint minimization procedure after the technical parameters of optimization have been properly adjusted (MathWorks, 2016); a special, user-defined function *normT7_prodT*(***gT***) recovers matrix $\boldsymbol{T}$ of pattern (C1) from its vector argument $\boldsymbol{gT} \in \mathbb{R}_+^7$ and calculates the norm of difference $\boldsymbol{T}^7 - \boldsymbol{prodT}$, where ***prodT*** is the product of 7 matrices $\boldsymbol{T}_t$ in the chronological order (matrices do no commute in the product); vector $\boldsymbol{gT0} \in \mathbb{R}_+^7$ is the starting point of the searching algorithm, the output argument $\boldsymbol{gT} \in \mathbb{R}_+^7$ is the (local) solution to the problem, *FVAL* is the corresponding minimal value of function *normT7_prodT*.

The global minimum of the approximation error equals 6.35487...× 10^{-5} and is attained when

$$\boldsymbol{T}_{\mathrm{gm}} = \begin{bmatrix} 0 & 0 & 0 & 0 & 0 \\ 0.221078 & 0 & 0 & 0 & 0 \\ 0.105263 & 0.354842 & 0.275318 & 0 & 0 \\ 0 & 0 & 0.217935 & 0.636621 & 0 \\ 0 & 0 & 0 & 0.090199 & 0 \end{bmatrix} \quad \text{(C4)}$$

(with an accuracy of 10^{-6}).

The following Matlab commands of logical comparison:

$$\gg \mathrm{round}(10\mathrm{e} + 6{*}\boldsymbol{gT}) == \mathrm{round}(10\mathrm{e} + 6{*}\min \boldsymbol{T}),$$
$$\mathrm{round}(10\mathrm{e} + 6{*}\boldsymbol{gT}) == \mathrm{round}(10\mathrm{e} + 6{*}\max \boldsymbol{T}),$$

return

$$\mathrm{ans} = 0\,1\,0\,0\,0\,0\,0, \quad \mathrm{ans} = 0\,0\,0\,0\,0\,0\,0,$$

so that the lower bound is achieved only by parameter d, while the upper bound is not reached at all.

ACKNOWLEDGMENTS

This study was supported in the field data mining part by the Russian Foundation for Basic Research, project no. 14-04-00214; in the modeling part by project nos. 13-04-01836 and 16-04-00832. Data processing and writing texts with the support by the Russian Science Foundation, project no. 14-50-00029.

COMPLIANCE WITH ETHICAL STANDARDS

Conflict of interests. The authors declare that they have no conflict of interest.

Statement on the welfare of animals. This article does not contain any studies with animals performed by any of the authors.

REFERENCES

Artyushenko, Z.T., *Atlas po opisatel'noi morphologii vysshikh rastenii: semya* (Atlas on Descriptive Morphology of Higher Plants: Seed), Leningrad: Nauka, 1990.

Bender, M.H., Baskin, J.M., and Baskin, C.C., Age of maturity and life span in herbaceous, polycarpic perennials, *Bot. Rev.*, 2000, vol. 66, no. 3, pp. 311–349.

Bernardelli, H., Population waves, *J. Burma Res. Soc.*, 1941, vol. 31, pp. 1–18.

Caswell, H., *Matrix Population Models: Construction, Analysis, and Interpretation*, Sunderland, MA: Sinauer Associates, 2001, 2nd ed.

Cochran, M.E. and Ellner, S., Simple methods for calculating age-based life history parameters for stage-structured populations, *Ecol. Monogr.*, 1992, vol. 62, no. 3, pp. 3455–3464.

Crone, E.E., Menges, E.S., Ellis, M.M., Bell, T., Bierzychudek, P., and Ehrlen, J., How do plant ecologists use matrix population models? *Ecol. Lett.*, 2011, vol. 14, pp. 1–8.

Crone, E.E., Ellis, M.M., Morris, W.F., Stanley, A., Bell, T., and Bierzychudek, P., Ability of matrix models to explain the past and predict the future of plant populations, *Conserv. Biol.*, 2013, vol. 27, pp. 968–978.

Cushing, J.M. and Yicang, Z., The net reproductive value and stability in matrix population models, *Nat. Resour. Model.*, 1994, vol. 8, no. 4, pp. 297–333.

Diemer, M., Population dynamics and spatial arrangement of *Ranunculus glacialis* L., an alpine perennial herb, in permanent plots, *Vegetatio*, 1992, vol. 103, no. 2, pp. 159–166.

Dinamika tsenopopulyatsii rastenii (Dynamics of Local Plant Populations), Moscow: Nauka, 1985.

Dobronets, B.S., *Intervalnaya matematika* (Interval Mathematics), Krasnoyarsk: Krasn. Gos. Univ., 2004.

Egorov A.V., Structure of species diversity in plant communities of the Teberda Nature Reserve. *Cand. Sci. (Biol.) Dissertation*, Moscow: Moscow State Univ., 2015.

Egorov, A.V., Onipchenko, V.G., and Tekeev, D.K., Habitat ecological properties of alpine plant species in Teberda Nature Reserve, *Tr. Teberdinsk. Gos. Zapoved.*, 2012, no. 52.

Fedorov, A.A., Kirpichnikov, M.A., and Artyushenko, Z.T., *Atlas po opisatel'noi morfologii vysshikh rastenii: list* (Atlas on the Descriptive Morphology of Higher Plants: Leaf), Moscow: Akad. Nauk SSSR, 1956.

Fedorov, A.A., Kirpichnikov, M.A., and Artyushenko, Z.T., *Atlas po opisatel'noi morfologii vysshikh rastenii: stebel' i koren'* (Atlas on the Descriptive Morphology of Higher Plants: Stem and Root), Moscow: Akad. Nauk SSSR, 1962.

Grime, J.P., *Plant Strategies and Vegetation Processes*, Chichester: Wiley, 1979.

Grime, J.P., *Plant Strategies, Vegetation Processes, and Ecosystem Properties*, Chichester: Wiley, 2001, 2nd ed.

Grossheim, A.A., *Flora Kavkaza* (Flora of the Caucasus), Leningrad: Nauka, 1967, vol. 7.

Harper, J.L. and White, J., The demography of plants, *Annu. Rev. Ecol. Syst.*, 1974, vol. 5, pp. 419–463.

Kazantseva, E.S., Population dynamics and seed productivity of short-lived alpine plants in the North-West Caucasus, *Cand. Sci. (Biol.) Dissertation*, Moscow: Moscow State Univ., 2016.

Kazantseva, E.S., Shulakov, A.A., and Kipkeev, A.M., Anthecology of three alpine plant species of North-West Caucasus, *Proc. XV Int. Sci. Conf. "Biodiversity of the Caucasus and Southern Russia," Makhachkala, November 5–6, 2013*, Makhachkala, 2013, pp. 264–265.

Kazantseva, E.S., Onipchenko, V.G., Kipkeev, A.M., and Rovnaya, E.N, Parameters of seed renewal of alpine juveniles and their comparison with perennial plants, *Byull. Mosk. O-va. Ispyt. Prir., Otd. Biol.*, 2016, vol. 121, no. 4, pp. 43–51.

Keller, R. and Vittoz, P., Clonal growth and demography of a hemicryptophyte alpine plant: *Leontopodium alpinum* Cassini, *Alp. Bot.*, 2014, vol. 125, no. 1, pp. 31–40.

Kemeny, J.G. and Snell, J.L., *Finite Markov Chains*, Berlin: Springer-Verlag, 1976.

Kipkeev, A.M., Onipchenko, V.G., Tekeev, D.K., Erkenova, M.A., and Salpagarova, F.S., Age of maturity in alpine herbaceous perennials in the North-West Caucasus, *Biol. Bull. Rev.*, 2015, vol. 5, no. 5, pp. 505–511.

Körner, C., *Alpine Plant Life: Functional Plant Ecology of High Mountain Ecosystems*, Berlin: Springer-Verlag, 2003, 2nd ed.

Krasnaya kniga Krasnodarskogo kraya (rasteniya i griby) (The Red Data Book of the Krasnodar Krai: Plants and Fungi), Litvinskaya, S.A., Ed., Krasnodar: Dizain Byuro, 2007, 2nd ed.

Krasnaya kniga Respubliki Adygeya: Redkiye i nakhodyashchiyesya pod ugrozoy ischeznoveniya ob''yekty zhivotnogo i rastitel'nogo mira. Chast' 1. Rasteniya i griby (The Red Data Book of the Adygea Republic: Rare and Endangered Objects of Fauna and Flora, Part 1: Plants and Fungi), Zamotailov, A.S., Ed., Maikop: Kachestvo, 2012, 2nd ed.

Kurashev, A.S., Anthecology of alpine plants in the North-Western Caucasus, *Cand. Sci. (Biol.) Dissertation*, Moscow: Moscow State Univ., 2012.

Leslie, P.H., On the use of matrices in certain population mathematics, *Biometrika*, 1945, vol. 33, pp. 183–212.

Lewis, E.G., On the generation and growth of a population, *Sankhya*, 1942, vol. 6, pp. 93–96.

Li, C.-K. and Schneider, H., Application of Perron–Frobenius theory to population dynamics, *J. Math. Biol.*, 2002, vol. 44, pp. 450–462.

Logofet, D.O., Convexity in projection matrices: projection to a calibration problem, *Ecol. Model.*, 2008, vol. 216, no. 2, pp. 217–228.

Logofet, D.O., Svirezhev's substitution principle and matrix models for dynamics of populations with complex structures, *Zh. Obshch. Biol.*, 2010, vol. 71, no. 1, pp. 30–40.

Logofet, D.O., Complexity in matrix population models: polyvariant ontogeny and reproductive uncertainty, *Ecol. Complexity*, 2013a, vol. 15, pp. 43–51.

Logofet, D.O., Projection matrices in variable environments: λ_1 in theory and practice, *Ecol. Model.*, 2013b, vol. 251, pp. 307–311.

Logofet, D.O., Projection matrices revisited: a potential-growth indicator and the merit of indication. *J. Math. Sci.*, 2013c, vol. 193, no. 5, pp. 671–686.

Logofet, D.O. and Belova, I.N., Nonnegative matrices as a tool to model population dynamics: classical models and contemporary expansions, *J. Math. Sci.*, 2008, vol. 155, no. 6, pp. 894–907.

Logofet D.O., Ulanova, N.G., and Belova, I.N., Adaptation on the ground and beneath: does the local population maximize its λ_1? *Ecol. Complexity*, 2014, vol. 20, pp. 176–184.

Logofet, D.O., Ulanova, N.G., and Belova, I.N., Polyvariant ontogeny in woodreeds: novel models and new discoveries, *Biol. Bull. Rev.*, 2016, vol. 6, no. 5, pp. 365–385.

Logofet D.O., Ulanova, N.G., and Belova, I.N., From uncertainty to an exact number: developing a method to estimate the fitness of a clonal species with polyvariant ontogeny, *Biol. Bull. Rev.*, 2017a, vol. 7, no. 5, pp. 387–402.

Logofet, D.O., Belova, I.N., Kazantseva, E.S., and Onipchenko, V.G., Local population of *Eritrichium caucasicum* as an object of mathematical modeling. I. Life cycle graph and a nonautonomous matrix model, *Biol. Bull. Rev.*, 2017b, vol. 7, no. 5, pp. 415–427.

Logofet, D.O., Kazantseva, E.S., Belova, I.N., and Onipchenko, V.G., Local population of *Eritrichium caucasicum* as an object of mathematical modeling. II. How short does the short-lived perennial live?, *Biol. Bull. Rev.*, 2018, vol. 8, no. 3, pp. 193–202.

Markov, M.V., *Populyatsionnaya biologiya rastenii* (Population Biology of Plants), Moscow: KMK, 2012.

Mirkin, B.V. and Naumova, L.G., *Nauka o rastitel'nosti (istoriya i sovremennoye sostoyaniye osnovnykh kontseptsiy)* (The Science on Vegetation: History and Current State of the Basic Concepts), Ufa: Gilem, 1998.

Molisch, H., *The Longevity of Plants* (Die Lebensdauer der Pflanze), New York: E.H. Fulling, 1938.

Nakhutsrishvili, G.S. and Gamtsemlidze, Z.G., *Zhizn' rastenii v extremal'nykh usloviyakh vysokogorii: na primere Tsentral'nogo Kavkasa* (Plant Life in Extreme High-Altitude Conditions by Example of the Central Caucasus), Leningrad: Nauka, 1984.

Onipchenko, V.G., *Alpine Vegetation of the Teberda Nature Reserve, the Northwest Caucasus* (Veröffentlichungen des Geobotanischen Institutes der Eidgenössische Technische Hochschule), Zurich: Stiftung Rübel, 2002, no. 130.

Onipchenko, V.G., *Funktsional'naya fitotsenologiya: sinekologiya rasteniy* (Functional Phytocenology: Synecology of the Plants), Moscow: Krasand, 2013.

Onipchenko, V.G. and Komarov, A.S., Population dynamics and life history features of three alpine plant species in the Northwest Caucasus, *Zh. Obshch. Biol.*, 1997, vol. 58, no. 6, pp. 64–75.

Onipchenko, V.G., Zernov, A.S., and Vorob'eva, F.M, Vascular plants of the Teberda Nature Reserve: annotated list of species, in *Flora i fauna zapovednikov* (Flora and Fauna of Nature Reserves), Moscow: Inst. Probl. Ekol. Evol., Ross. Akad. Nauk, 2011, no. 99A.

Pavlov, V.N. and Onipchenko, V.G., High altitude vegetation, *Itogi Nauki Tekh., Ser.: Bot.*, 1987, vol. 7, pp. 3–38.

Pierce, S., Negreiros, D., Cerabolini, B.E.L., et al., A global view and measurement of plant ecological strategies from leaf economics and size traits, *Funct. Ecol.*, 2017, vol. 31, no. 2, pp. 444–457.

Polevaya geobotanika (Field Geobotany), Lavrenko, E.M. and Korchagin, A.A., Eds., Moscow: Akad. Nauk SSSR, 1960, vol. 2.

Polivariantnost' razvitiya organizmov, populyatsii i soobshchestv (Polyvariant Development of Organisms, Populations, and Communities), Yoshkar-Ola: Mariisk. Gos. Univ., 2006.

Popova, A.S., Biology of short-lived alpine plants (exemplified with the Teberda Nature Reserve), *MSc Dissertation*, Pushchino, 2010.

Populyatsionnaya ekologiya i introduktsiya rastenii (Population Ecology and Introduction of the Plants), Semkina, L.A. and Mamaeva, S.A., Eds., Yekaterinburg: Ural. Fil., Ross. Akad. Nauk, 2003, no. 2.

Rabotnov, T.A., Duration of the virgin period in the life span of herbaceous perennials in natural conenoses, *Byull. Mosk. O-va. Ispyt. Prir., Otd. Biol.*, 1946, vol. 51, no. 2, pp. 41–48.

Rabotnov, T.A., The life cycle of perennial herbaceous plants and their population structures, *Nauchno-Metod. Zap. Glav. Uprav. Zapoved. RSFSR*, 1949, no. 12, pp. 91–98.

Rabotnov, T.A., Life cycle of perennial herbaceous plants in meadow phytocenosises, *Tr. Bot. Inst., Akad. Nauk SSSR, Ser. 3. Geobot.*, 1950a, no. 6, pp. 7–204.

Rabotnov, T.A., The phytocenological analysis of the population structure, *Probl. Bot.*, 1950b, no. 1, pp. 465–483.

Salguero-Gómez, R., Jones, O.R., Archer, C.A., et al., The COMPADRE plant matrix database: an online repository for plant population dynamics, *J. Ecol.*, 2015, vol. 103, pp. 202–218.

Semenova, G.V. and Onipchenko, V.G., Soil seed bank of an alpine lichen heath in the Northwestern Caucasus: species richness, *Oecol. Mon.*, 1996, vol. 5, no. 2, pp. 83–86.

Shetekauri, Sh., Spatial distribution characteristics of glacial relief flora in the high mountains of the Caucasus, *Feddes Repertorium*, 1998, vol. 109, pp. 465–472.

Shidakov, I.I. and Onipchenko, V.G., Comparative analysis of alpine plant leaf traits in the Teberda Nature Reserve, *Byull. Mosk. O-va Ispyt. Prir., Otd. Biol.*, 2007, vol. 112, no. 4, pp. 42–50.

Shishkin, B.K. and Bobrov, E.G., *Androsace* genus, in *Flora SSSR* (Flora in the USSR), Shishkin, B.K. and Bobrov, E.G., Eds., Moscow: Akad. Nauk SSSR, 1952, vol. 18, pp. 221–243.

Shkhagapsoev, S.Kh., *Morfostruktura podzemnykh organov rastenii pervichnoobnazhennykh sklonov Kabardino-Balkarii* (Morphological Structure of the Underground Organs of Plants on the Primary Slopes of Kabardino-Balkaria), Nalchik: Kabardino-Balkar. Gos. Univ., 1999.

Sizov, I.E., Onipchenko, V.G., and Komarov, A.S., Life span indirect evaluation of three alpine perennial plants, *Oecol. Mo.*, 1999, vol. 8, nos. 1–2, pp. 21–26.

Sovremennye podkhody k opisaniyu struktury rasteniya (Modern Approaches to Description of the Plant Structures), Savinykh, N.P. and Bobrovykh, Yu.A., Eds., Kirov: Loban', 2008.

Tsenopopulyatsii rastenii: osnovnye ponyatiya i struktura (Plant Cenopopulations: General Terms and Structure), Uranov, A.A. and Serebryakova, T.I., Eds., Moscow: Nauka, 1976.

Uranov, A.A., Age spectrum of phytocoenopopulations as a function of time and energetic wave processes, *Biol. Nauki*, 1975, no. 2, pp. 7–34.

Vorob'eva, F.M. and Onipchenko, V.G., Vascular plants of Teberda Nature Reserve, in *Flora i fauna zapovednikov* (Flora and Fauna of Nature Reserves), Gubanov, I.A., Ed., Tula: Grif i K, 2001, no. 99, pp. 1–100.

Witte de, L.C. and Stöcklin, J., Longevity of clonal plants: why it matters and how to measure it, *Ann. Bot.*, 2010, vol. 106, pp. 859–870.

Zernov, A.S., *Flora Severo-Zapadnogo Kavkaza* (Flora of the Northwest Caucasus), Moscow: KMK, 2006.

Zernov, A.S., *Opredelitel' sosudistykh rastenii Karachaevo-Cherkesskoi Respubliki* (Guide for Identification of Vascular Plants of the Karachay-Cherkessia Republic), Moscow: KMK, 2015.

Zhmylev, P.Yu., Alekseev, Yu.E., Karpukhina, E.A., and Balandin, S.A., *Biomorfologiya rastenii: illustrirovannyi slovar'* (Plant Biomorphology: Illustrated Dictionary), Tula: Grif i K, 2005, 2nd ed.

Zhukova, L.A., Polyvariance of the meadow plants, in *Zhiznennye formy v ekologii i sistematike rastenii* (Life Forms in Ecology and Plant Systematics), Moscow: Mosk. Gos. Pedagog. Inst., 1986, pp. 104–114.

Zhukova, L.A., *Populyatsionnaya zhizn' lugovykh rastenii* (Population Life of Meadow Plants), Yoshkar-Ola: Lanar, 1995.